Performance analysis of DAST material assisted electro-optically tuned Bloch surface wave sensor

Performance Analysis of DAST Material Assisted Electro-optically Tuned Bloch Surface Wave Sensor

Amit Kumar Goyal and Yehia Massoud, *Fellow, IEEE*
Innovative Technologies Laboratories (ITL), King Abdullah University of Science and Technology (KAUST), Thuwal, Saudi Arabia - 23955
***** Correspondence: yehia.massoud@kaust.edu.sa

ABSTRACT

In this manuscript, a 4-N, N-dimethylamino-4′ -N′ -methyl-stilbazolium tosylate (DAST) material assisted electro-optically tuned Bloch Surface Wave Sensor is proposed. The structure is designed using a one-dimensional photonic crystal (1D-PhC) structure. A top defective layer of DAST as an electro-optic material is used. The analysis shows that by illuminating the device with poly-chromatic light at an incident angle of 45.11° results in Bloch mode excitation at a 632.8nm operating wavelength. The analytical results also demonstrate the post fabrication 47 nm BSW wavelength tuning by applying only ±5 V potential. The structure also exhibits both wavelength stability (at varying angle) and angular stability (at varying wavelength). Moreover, the structure exhibits 105.71nm/RIU sensitivity at 0V applied bias voltage having very low FWHM of <1nm. Thus, the proposed design possesses the advantage in terms of low voltage wavelength tuning, stable response, easy fabrication, and integration capability in integrated circuits.

Keyword: Bloch Surface Wave, Electro-optical Material, DAST, Tunable Surface Wave

1. INTRODUCTION

Recently, post fabrication optical properties tunning of the surface wave-based nano-photonic devices working in visible region are growing interest because of their inherent properties of higher field confinement with very narrow full-width-at-half-maximum (FWHM).[1-3] The Bloch surface wave (BSW) based devices are considered equivalent to surface plasmon devices, having better performance characteristics.[4-6] The tunability in BSW mode excitation can be achieved by introducing functional materials such as thermo-optical, chromic, and electro-optical materials along with conventional one-dimensional photonic crystal (1D-PhC) structure.[7-9] Among these, electro-optical (EO) tunning is considered to have fast switching. Recently in 2022 Farhadi et al, tune the operating frequency and localization of surface waves by varying the Fermi energy of Dirac semimetal defect layer.[10] Similarly, Chikhi et al., used a nanocomposite defect layer to tune the performance of BSW biosensor.[11]

In this paper, a very simple electrically tunable Bloch Surface Wave (BSW) device structure is proposed. The device is designed considering one-dimensional photonic crystal (1D-PhC) structure having SiO_2 and TiO_2 materials to form the 1D-PhC having an organic crystal 4-N, N-dimethylamino-4'-N'-methyl-stilbazolium tosylate (DAST) material as a top defect layer. The insertion of DAST defect layer facilitates the excitation of BSW mode at the top interface. Here, we are considering DAST material because it possesses very large EO-coefficient (3.41 nm/V).[12] The design optimization is carried out using transverse Matrix method,[13-15] where electrical field profile of incident, reflected and transmitted field is measured to calculate the corresponding reflection and transmission coefficient.[16-18] The structural analysis depicts that by incidenting a polychromatic light at 45.11° incidence angle results in excitation of BSW mode. We also evaluated the impact of defect layer thickness of BSW excitation characteristic and finally impact of applied bias voltage of proposed device is evaluated. The results shows that the device exhibits excellent electrical tuning in excited BSW mode wavelength by just applying ±5V bias voltage. Moreover, the structure also shows its sensing capability at these applied bias voltages, thus showing its capabilities to be used as a tunable BSW sensing devices.

2. STRUCTURE DESIGN

The structure is designed considering SiO_2 and TiO_2 materials having physical (refractive index) thickness 85nm (n = 2.2) and 128nm (n = 1.46), whereas 100nm thick DAST material is considered as top defect layer a shown in Fig. 1. The lossy nature of material is also considered by using imaginary dielectric constant of around 0.0002i and 0.0001i respectively. The refractive index of DAST ($n_D = n_0 + \frac{dn}{du} \times \frac{V}{d_D}$) is taken from literature.[19] Here, 'n_0' represents the DAST refractive index for without any bias voltage (here, 2.2), 'V' is the applied voltage, $\frac{dn}{du}$ is EO coefficient of DAST (3.41 nm/V) and, 'd_D' is the physical thickness of DAST material. The parameters are optimized to excite the BSW mode at an operating wavelength of 632.8nm for the considered structure 'Glass|$(TiO_2,SiO_2)^7$|DAST|air'.

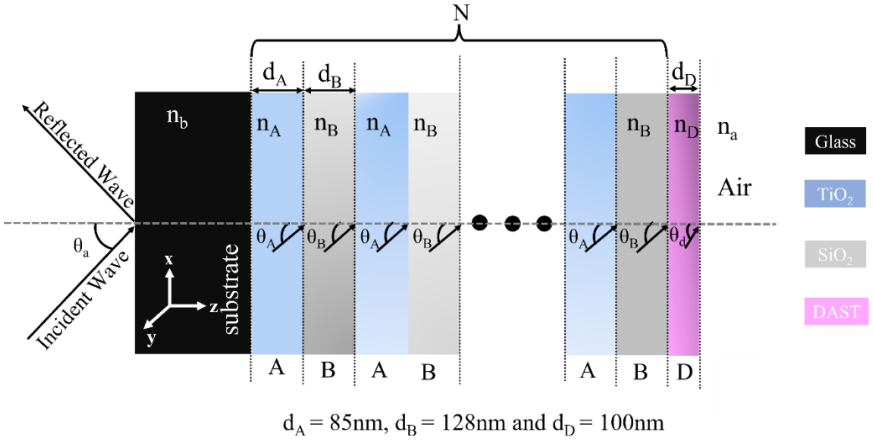

d_A = 85nm, d_B = 128nm and d_D = 100nm

Figure 1. Schematical illustration of proposed 1D-PhC structure 'Glass|$(TiO_2, SiO_2)^7$|DAST|Air

3. RESULTS AND DISCUSSIONS

The proposed structure shows an excellent excitation of BSW mode at an incidence angle of 45.07° at 632.8nm operating wavelength. However, the incidence angle and operating wavelength to excite these BSW modes are highly depends on defect layer thickness. Therefore, the impact of DAST layer thickness on BSW excitation is evaluated by wavelength interrogation method and is represented in Fig. 2. Figure 2(a) shows the wavelength dispersion characteristics to study the effect of DAST layer thickness variation on generation of BSW at fixed incidence angle of 45.07°. The defect layer thickness is increased in the range of 80nm - 200nm with the increment of 0.5nm.

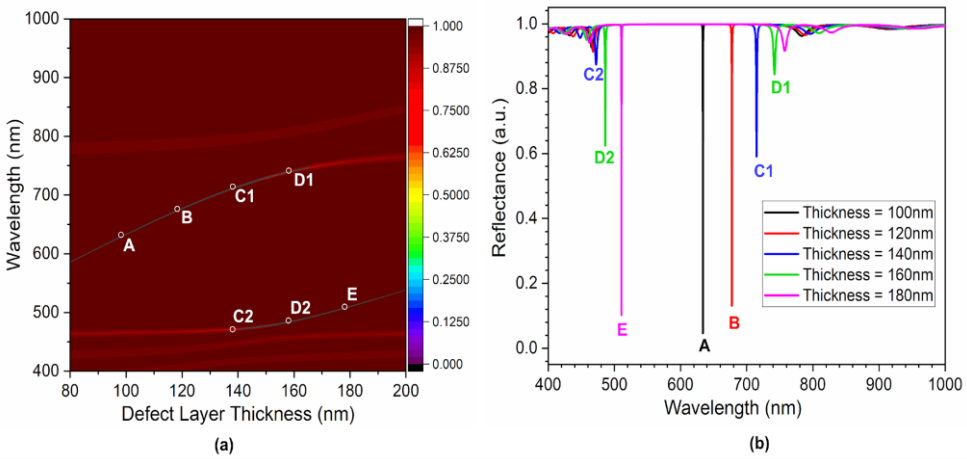

Figure 2. Effect of defect layer thickness on generation of BSW at fixed incidence angle of 45.07° (a) Dispersion characteristic and, (b) Reflection spectrum.

It can be seen in wavelength dispersion characteristics of Fig. 2(a) that for a fixed incidence angle the structure shows excitation of several surface modes for different combinations of operating wavelengths and DAST layer thicknesses. This is represented by a solid line in Fig. 2(a). We have considered discrete five points (A-E) corresponds to 100nm, 120nm, 140nm, 160nm, and 180nm thickness of DAST material. This leads to BSW mode excitation at corresponding mode wavelengths of 632.8nm, 677.51nm, 714.87nm, 741.93nm and 757.53nm, respectively. The structure also shows excitation of dual frequency surface modes for point 'C' and 'D'. The lower energy surface modes dominate for a defect layer thickness of less than 140nm, whereas higher energy modes dominate afterward. The modes 'C2' and 'D1' are coupled to leaky modes thus are not considered as surface mode. The structure shows excitation of stable surface modes (modes 'A', 'B', 'C1' 'D2' and 'E') for corresponding defect material thickness of 100 nm, 120 nm, 140 nm, 160 nm, and 180 nm as shown in Fig. 2(b). The carried analysis reveals that the device possesses a high fabrication tolerance because even having variation in defect layer thickness, a surface mode is still excited. Similarly, the angular interrogation is also carried out to study the device characteristics at a constant operating wavelength, which shows around 24° variation in incidence angle for corresponding 100nm-180nm change in DAST layer thickness.

$$\lambda_{BSW} = 632.8\,(\pm 0.022) + 4.733(\pm 0.0046) \times V - 0.0943(\pm 0.0016) \times V^2 \quad (1)$$

Further, the impact of bias voltage is evaluated for the proposed structure. Applying the bias voltage leads to change the refractive index of material, which results in change in operating wavelength (incidence angle) of excited BSW at fixed incidence angle (or fixed operating wavelength). For this, a bias voltage of ±5V with the step of 0.1V is applied and corresponding angular dispersion and wavelength dispersion characteristics is measured. Applying the bias voltage leads to strong BSW excitation however, the required operating wavelength or incidence angle to excite BSW is red shifted. The analysis shows a 5.5° incidence angle tunning at fixed operating wavelength of 632.8nm and 47nm operating wavelength tuning at fixed incidence angle of 45.07°. The voltage dependent structure response can be calculated by equation 1.

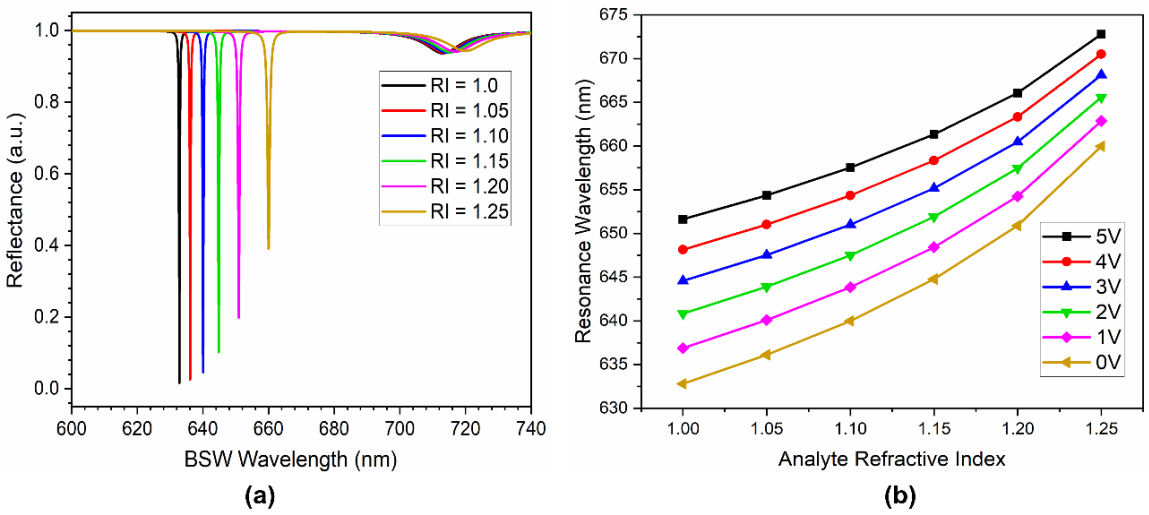

Fig. 3: The wavelength sensing interrogation of proposed structure having DAST layer thickness of 140nm and incidence angle 58.04° (a) The impact of varying analyte refractive indices on excited surface wave wavelength for 0V applied bias voltage and, (b) Corresponding voltage dependent tunable sensing response.

Finally, the voltage dependent sensitivity analysis of proposed structure 'Glass|(TiO_2, SiO_2)^7|DAST|analyte' having 140nm DAST thickness, is carried out by infiltrating the analyte of varying refractive index (1.0 – 1.25). The wavelength interrogation is carried out at constant incidence angle of 58.04° and corresponding reflectance response is shown in Fig 3(a). The performance parameters like sensitivity ($S = \frac{\Delta\lambda}{\Delta n}$; $S = \frac{\Delta\theta}{\Delta n}$), and figure-of-merit (FOM= S/FWHM) of the structure are calculated[20,21]. Further, the bias voltage is applied from 0V to 5V with the step of 1V and corresponding sensing response of proposed design is measured. Increasing the applied bias voltage leads to sensing performance variation as represented in Fig. 3(b) and this can be calculated by equation 2.

$$S = 105.71329(\pm 0.02253) - 4.6357(\pm 0.02119) \times V + 0.00704(\pm 0.00407) \times V^2 \quad (2)$$

Where, 'S' is representing the voltage dependent sensitivity of the proposed structure. The equation 2 is obtained by polynomial curve fitting of the Fig. 3(b) having coefficients of determination R^2 of around 0.99999. The structure shows an average angular and wavelength sensitivity of around 17.51°/RIU and 105.71nm/RIU, respectively without any bias voltage. Moreover, it exhibits a FWHM of less than 1nm. This results in an average FOM of around 372.4 RIU^{-1}. The structure demonstrates a comparative sensing performance having much better FOM than recently reported values. Therefore, the proposed structure demonstrates its capability as electro-optical tunable surface wave generation and refractive index sensors.

4. CONCLUSION

The manuscript presents a DAST material assisted dynamic tunning of Bloch surface mode. The one-dimensional photonic crystal (1D-PhC) structure of the device is designed with SiO_2 and TiO_2 materials along with DAST material as a top defect layer. The analysis shows that by illuminating the device with poly-chromatic light at an incident angle of 45.11° results in Bloch mode excitation at a 632.8nm operating wavelength. Further, by using the electro-optical property of DAST material, the mode excitation wavelength can be dynamically tunned by 47nm. The structure also exhibits both wavelength stability (at varying angle) and angular stability (at varying wavelength). Thus, the proposed design possesses the advantage in terms of low voltage wavelength tuning, stable response, easy fabrication, and integration capability in integrated circuits.

ACKNOWLEDGEMENT

The authors would like to acknowledge the research funding to the Innovative Technologies Laboratories (ITL) from King Abdullah University of Science and Technology (KAUST).

REFERENCES

1. Neubrech, F.; Duan, X.; Liu, N. Dynamic plasmonic color generation enabled by functional materials. Sci. Adv. 2020, 6, eabc2709.
2. Du K; Barkaoui H; Zhang X; Jin L; Song Q; Xiao S. Optical metasurfaces towards multifunctionality and tunability. Nanophotonics 2021.
3. Goyal, A.K.; Kumar, A.; Massoud, Y. Performance Analysis of DAST Material-Assisted Photonic-Crystal-Based Electrical Tunable Optical Filter. *Crystals* **2022**, *12*, 992. https://doi.org/10.3390/cryst12070992
4. Goyal, A.K., Pal, S. Design analysis of Bloch surface wave-based sensor for haemoglobin concentration measurement. Appl Nanosci 10, 3639–3647 (2020).
5. L. Yu, E. Barakat, T. Sfez, L. Hvozdara, J. Di Francesco, H.P. Herzig, "Manipulating Bloch surface waves in 2D: a platform concept-based flat lens," LIGHT-SCI APPL 3, 124 (2014).
6. Goyal, A.K.; Saini, J. Performance Analysis of Bloch Surface Wave Based Sensor using Transition Metal Dichalcogenides. *Appl. Nanosci.* **2020**, *10* 4307–4313.
7. H. Hajian, B. Rezaei, A. Soltani Vala, M. Kalafi, Tuned switching of surface waves by a liquid crystal cap layer in one-dimensional photonic crystals, Appl. Opt. 51 (2012) 2909–2916.
8. Wuttig, M.; Bhaskaran, H.; Taubner, T. Phase-change materials for non-volatile photonic applications. *Nat. Photonics* **2017**, *11*, 465.
9. X. Wu, E. Barakat, L. Yu, L. Sun, J. Wang, Q. Tan, H.P. Herzig, "Phase-sensitive near field Investigation of Bloch surface wave propagation in curved waveguides," JEOS:RP 9, 14049 (2014).
10. P. Farhadi, B. Rezaei, Tunable terahertz Bloch surface waves in one-dimensional photonic crystals with a Dirac semimetal cap layer, Optik, 265 (2022) 169538.
11. Malika Chikhi, Fouzia Boukabrine, and Nadia Benseddik, High-Sensitivity Tunable Bloch Surface Waves' Biosensor Using Nanocomposite Cap Layer, Phys. Status Solidi A 2022, 219, 2100607.
12. Stepanov, A.G.; Bonacina, L.; Wolf, J. DAST/SiO2 multilayer structure for efficient generation of 6 THz quasi-single-cycle electromagnetic pulses. Opt. Lett. 2012, 37, 2439–2441

13. A. Hosseini, Y. Massoud, “Optical range microcavities and filters using multiple dielectric layers in metal-insulator-metal structures, “JOSA A 24 (1), 221-224, 2007
14. Amit Kumar Goyal, HS Dutta, S Pal, “Development of uniform porous one-dimensional photonic crystal based sensor,” Optik, 223, 165597 (2020).
15. A. Hosseini, H. Nejati, and Y. Massoud, “Modeling and design methodology for metal-insulator-metal plasmonic Bragg reflectors, “Optics express 16 (3), 1475-1480, 2008
16. A. Hosseini and Y. Massoud, “A low-loss metal-insulator-metal plasmonic bragg reflector, “Optics express 14 (23), 11318-11323, 2006
17. A. Hosseini, H. Nejati, and Y. Massoud, “Design of a maximally flat optical low pass filter using plasmonic nanostrip waveguides,” Optics Express 15 (23), 15280-15286, 2007
18. Goyal, A.K.; Massoud, Y. Interface Edge Mode Confinement in Dielectric-Based Quasi-Periodic Photonic Crystal Structure. Photonics 2022, 9, 676. https://doi.org/10.3390/photonics9100676
19. Jazbinsek, M.; Mutter, L.; Gunter, P. Photonic applications with the organic nonlinear optical crystal DAST. IEEE J. Sel. Top. Quantum Electron. 2008, 14, 1298–1311.
20. Goyal, A.K.; Kumar, A.; Massoud, Y. Thermal Stability Analysis of Surface Wave Assisted Bio-Photonic Sensor. Photonics 2022, 9, 324. https://doi.org/10.3390/photonics9050324
21. Amit Kumar Goyal, "Design Analysis of One-Dimensional Photonic Crystal Based Structure for Hemoglobin Concentration Measurement," Progress In Electromagnetics Research M, Vol. 97, 77-86, 2020.